

UC Irvine

UC Irvine Previously Published Works

Title

Performance Assessment of Turbocharged Pem Fuel Cell Systems for Civil Aircraft Onboard Power Production

Permalink

<https://escholarship.org/uc/item/9wg234vb>

Journal

Journal of Engineering for Gas Turbines and Power, 130(2)

ISSN

0742-4795

Authors

Campanari, Stefano
Manzolini, Giampaolo
Beretti, Andrea
et al.

Publication Date

2008-03-01

DOI

10.1115/1.2772636

Copyright Information

This work is made available under the terms of a Creative Commons Attribution License, available at <https://creativecommons.org/licenses/by/4.0/>

Peer reviewed

Performance Assessment of Turbocharged Pem Fuel Cell Systems for Civil Aircraft Onboard Power Production

Stefano Campanari

Associate Professor
e-mail: stefano.campanari@polimi.it

Giampaolo Manzolini

Research Engineer
e-mail: giampaolo.manzolini@polimi.it

Andrea Beretti

Research Engineer

Dipartimento di Energetica,
Politecnico di Milano,
Piazza Leonardo da Vinci 32,
20133 Milano, Italy

Uwe Wollrab

Systems Engineering,
Fuel Cell Systems Development,
AIRBUS Deutschland GmbH,
21129 Hamburg, Germany
e-mail: uwe.wollrab@airbus.com

In recent years, civil aircraft projects are showing a continuous increase in the demand of onboard electrical power, both for the partial substitution of hydraulic or pneumatic controls and drives with electrical ones, and for the consumption of new auxiliary systems developed in response to flight safety and environmental control issues. Aiming to generate onboard power with low emissions and better efficiency, several manufacturers and research groups are considering the possibility to produce a relevant fraction of the electrical power required by the aircraft by a fuel cell system. The first step would be to replace the conventional auxiliary power unit (based on a small gas turbine) with a polymer electrolyte membrane (PEM) fuel cell type, which today is favored with respect to other fuel cell types; thanks to its higher power density and faster startup. The PEM fuel cell can be fed with a hydrogen rich gas coming from a fuel reformer, operating with the same jet fuel used by the aircraft, or relying on a dedicated hydrogen storage onboard. The cell requires also an air compression unit, where the temperature, pressure, and humidity of the air stream feeding the PEM unit during land and in-flight operation strongly influence the performance and the physical integrity of the fuel cell. In this work we consider different system architectures, where the air compression system may exploit an electrically driven compressor or a turbocharger unit. The compressor type and the system pressure level are optimized according to a fuel cell simulation model, which calculates the cell voltage and efficiency as a function of temperature and pressure, calibrated over the performances of real PEM cell components. The system performances are discussed under different operating conditions, covering ground operation, and intermediate and high altitude cruise conditions. The optimized configuration is selected, presenting energy balances and a complete thermodynamic analysis.

[DOI: 10.1115/1.2772636]

1 Introduction

New projects of civil aircrafts are in these years frequently influenced by a development strategy focusing on more electric aircraft (MEA) or even all electric aircraft (AEA) concepts. The partial substitution of conventional hydraulic or pneumatic controls and drives with electrical ones (see Table 1), and the introduction of new auxiliary systems bring about an increase in onboard electric power consumption, reaching values around 560 kW for airplanes such as the B777 or A330/A340, and going toward 1.3–1.5 MW for next generation aircrafts [1–5].

Furthermore, the possible elimination of power offtakes from the main engines would increase the nominal power output required by a separated onboard electricity generator.

It is well known that a fraction of electric power is generated on-board civil aircrafts by small turbine units, acting as auxiliary power units (APUs). Such machines operate with simple cycle, uncooled operation, low turbine inlet temperature (TIT), and pressure ratio, generally with single stage radial compressor and a power output in the range of several tenth kilowatts and up to the hundred kilowatt scale. Their advantages include low weight, rapid startup, and robustness; disadvantages are primarily the low efficiency (15–18%) and significant NO_x and CO emissions. The

possible removal of power offtakes from the main engines would increase the nominal power of the APU system, making more important to look for higher efficiency and lower pollution devices.

Polymer electrolyte membrane fuel cells (PEM FCs) on their own are widely experimented in prototypes and generally recognized very attractive for future application in the automotive field; thanks to their ability to generate electricity with high efficiency (e.g., 50–55%) in tenth-kilowatt scale systems fed with hydrogen and operating at low temperatures (60–70°C). They also show a rather high power density (in terms of kW/kg and kW/dm³), fast startup, and negligible emissions. The quick development of this technology has suggested to consider their application also in the aeronautic field, within the perspective of a step by step development, which could also represent a new possible market for the beginning of their commercialization.

The technology roadmap for this development includes several steps, where the first should be introducing a pure hydrogen PEM system with minor aircraft changes, aiming to provide a fraction of electric power (well below the potential power requirements shown in Table 1) for auxiliary loads and emergency systems actually sustained by APUs and other generators (for instance, the air turbine that is used to drive the pumps of the emergency hydraulic circuit). Subsequent steps could involve the use of onboard reformers [3] as well as different FC types with increasing power output.

The concept of integrating a PEM unit onboard civil aircrafts has been already introduced in several works [2,6,7], where the fuel cell has been generally considered as a device with assigned

Contributed by the International Gas Turbine Institute of ASME for publication in the JOURNAL OF ENGINEERING FOR GAS TURBINES AND POWER. Manuscript received April 28, 2007; final manuscript received May 9, 2007; published online February 29, 2008. Review conducted by Dilip R. Ballal. Paper presented at the ASME Turbo Expo 2007: Land, Sea and Air (GT2007), Montreal, Quebec, Canada, May 14–17, 2007, Paper No. GT2007-27658.

Table 1 Actual and future electric consumptions, active in-flight or during ground operation, for large aircrafts. Values with parentheses are related to systems active in emergency only

Main electrical consumers	System architecture			System power (kW)
	Conventional	MEA	AEA	
Emergency pumps	(X)	(X)	(X)	(30)
Aux. hydraulic pumps	X	X	X	60
Fuel pumps	X	X	X	10
Ice and rain protection	X	X	X	10
Lighting	X	X	X	15
Commercial loads	X	X	X	25
Avionics	X	X	X	10
Galley	X	X	X	75
Cargo doors	—	X	X	15
Flight control	—	—	X	80
Landing gear	—	—	X	25
Engine starter	—	X	X	350
Wing antiice	—	—	X	200
Environmental and cooling system (ECS)	—	X	X	400
Total demand (kW)	205 (235)	970 (1000)	1275 (1305)	
In-flight demand (kW)	205	605	910	

energy balances. The scope of this paper is to discuss with better detail the possible plant configurations and the optimization of the FC operating conditions, using a model which takes into account the effects of variable fuel cell performances.

The PEM fuel cell requires to be fed with a high purity hydrogen fuel and with air; both reactants shall be properly humidified to allow an efficient and durable operation of the cell membrane, which works efficiently when wet. By the point of view of the cell operating conditions, pressurization increases the cell efficiency and power output (for a given fuel consumption), but is energetically expensive because the air flow has to be compressed. If such compression is carried out without recovering useful power from the cell pressurized exhausts, the compressor power consumption is higher than the power gain by the FC, so the final effect on the system is negative. For this reason, PEM systems usually work at pressure between 1.2 bars and 1.5 bars.

Conversely, when operating at high altitude and low ambient temperature, a certain degree of pressurization is necessary to allow the presence of liquid water at the cell typical operating temperatures. In such conditions, it becomes important to exploit the expansion of the cell exhaust gases with a turbine, leading to a turbocharged cell design. In all cases, it is therefore necessary to define the optimal pressure level of the fuel cell system and the most suitable system arrangement, which can be used to obtain the cell pressurization.

In the first section of the paper, a model for predicting the performances of PEM fuel cell, with variable pressure operation and hydrogen feeding, is discussed. Calculations are performed based on state-of-the-art performances of small PEM fuel cell stacks. Subsequently, two system arrangements are investigated, where the PEM system is pressurized by (i) an electrically driven compressor or (ii) a turbocharger unit, with (iii) an eventual burner ahead the turbine. This work presents a detailed analysis of the fuel cell operating parameters and of the other component characteristics (pressure drops and efficiencies), together with their effects on the system efficiency. The performances of such a system are predicted, evidencing the most suitable solution.

The option of integrating the PEM system with an eventual fuel reformer—capable of producing onboard the hydrogen required by the fuel cell, thus relying only on a jet fuel supply—is not addressed in this work, where we prefer to focus on the issues of integrating the PEM and the air compression unit. However, the option of storing hydrogen onboard is frequently regarded as pos-

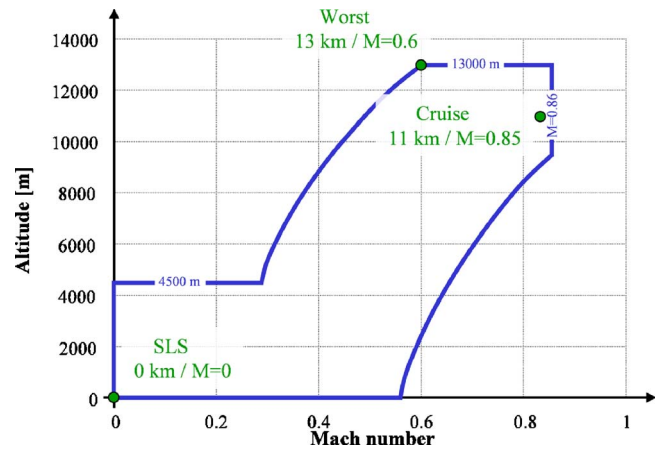


Fig. 1 Operating range that must be satisfied by an APU

sible in the mid- and long-term future, a time scale appropriate also for the eventual use of such kind of fuel cell systems.

2 Operating Conditions

The onboard PEM system shall work under variable ambient conditions during the aircraft flight. A typical operating range is shown in Fig. 1. We consider here three representative conditions (see dots in figure): ground operation, cruise conditions, and high altitude, low speed flight (the last called “worst” condition).

The following table (Table 2) shows the ambient conditions in the three cases. As already mentioned, the pressure level of the PEM system shall allow the presence of liquid water (avoiding the risk of boiling). Within a hypothesis of maximum cell local temperature of 80–85°C, the minimum tolerable pressure would be close to 0.57 bar according to water saturation tables; considering possible pressure oscillations, startup, and dynamic load variation issues, the design minimum pressure level can be set at 0.8 bar for the PEM system under flight conditions.

In all cases, we consider to design the fuel cell system for achieving a 60 kW net electric power output at cruise conditions, a value considered by preliminary projects at Airbus [4,8]; however, calculations may be easily extended to the case of a different power output.

3 Calculation Model

3.1 Fuel Cell Model. We make here reference to a PEM stack, which reflects the features of Nuvera fuel cell technology, with operating temperature of 70°C, which has been used for prototypes testing in the range of few kilowatt output as well as for hundred kilowatt-scale units [9].

The FC can be humidified by direct water injection (DWI) at the cathode, without requiring additional humidification at the anode side, because the amount of water used maintains the whole membrane humid, avoiding dehydration problems. The water stream can also act as the cell cooler by sensible heat exchange

Table 2 Selected operating conditions

	1 Ground	2 Cruise	3 Worst
Altitude (m)	0	11000	13000
Mach number	0	0.85	0.6
Static pressure (bar)	1.013	0.226	0.165
Pressure after dynamic inducer (bar)	0.974	0.268	0.182
Static temperature (K)	288.15	216.65	243.77
Temperature after dynamic inducer (K)	288.15	247.96	261.32

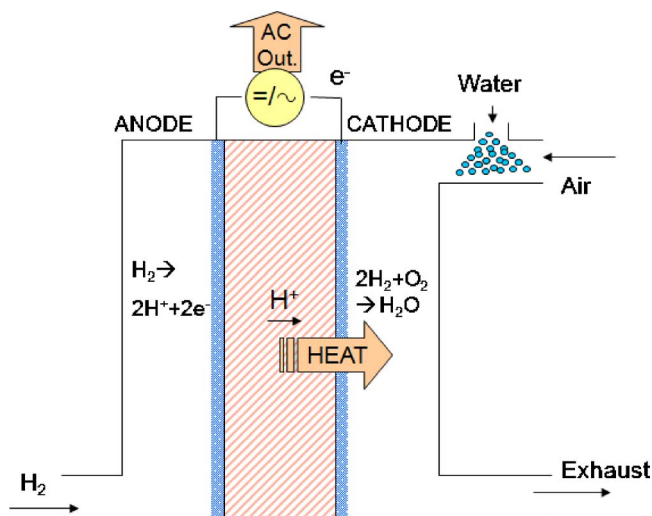


Fig. 2 PEM module operating principles and schematic layout

and partial evaporation, with the latter being the dominant effect [10]. Alternatively, the primary cooling effect can be carried out with a separated water loop, a solution preferred, for instance, for automotive applications; in this case, a water-glycol mixture circulates into cooling channels, which are inserted between adjoining cell groups; the coolant is then circulated in an air-cooled heat exchanger before returning to the FC [11,12]. The two options do not affect significantly the system energy balances discussed in this work; however, when applied to aircraft operation, both solutions have their drawbacks: (i) the DWI concept may suffer the pressure variations, which are experienced by the cell stack during real operation, requiring large variations of the amount of water sprayed at the cathode to obtain the cooling effect; moreover, evaporation becomes progressively inefficient when the stack pressure is increased above 1.5–2 bars, given that the cell average temperature cannot be increased above 75–80°C with actual membrane materials, so that heat exchange is primarily carried out by the liquid stream which increases its mass flow rate; (ii) the solution with a closed circuit cooling requires to adopt a saturator on the inlet air flow, which complicates the system layout; the saturator could be avoided during ground operation, but it becomes mandatory when operating with very dry inlet conditions, as typical when the FC is fed with compressed air during high altitude flight.

In this paper, we consider the first solution (cell cooling with water injection), presenting in some cases results of the second alternative. The PEM is fed by an oxidizer at the cathode (as mentioned, air mixed with water sprayed for humidification) and a fuel (Fig. 2). The two fluxes flow in contact with cathode and anode porous surfaces, separated by a solid membrane electrolyte, which is a good H⁺ ion conductor. The ionization of molecular hydrogen to H⁺ takes place at the anode, thanks to the effect of proper catalysts (generally platinum); hydrogen is then oxidized to steam at the cathode.

If the fuel at the anode inlet is pure hydrogen, as assumed in this paper, the PEM can work in a “dead-end” arrangement: the anode has only an entrance side and no exit (except for periodical purging of accumulated inerts and pressure regulation), and all the hydrogen is used in the fuel cell. If the fuel at the anode inlet is a mixture of hydrogen and other components, hydrogen can be electrochemically oxidized only up to a maximum fuel utilization factor, to avoid the large voltage losses due to reactant concentration gradients and limited gas diffusivity near the electrodes active area. The same consideration applies to the air flow; air and fuel utilization factors (see Nomenclature) quantify the consumed fractions.

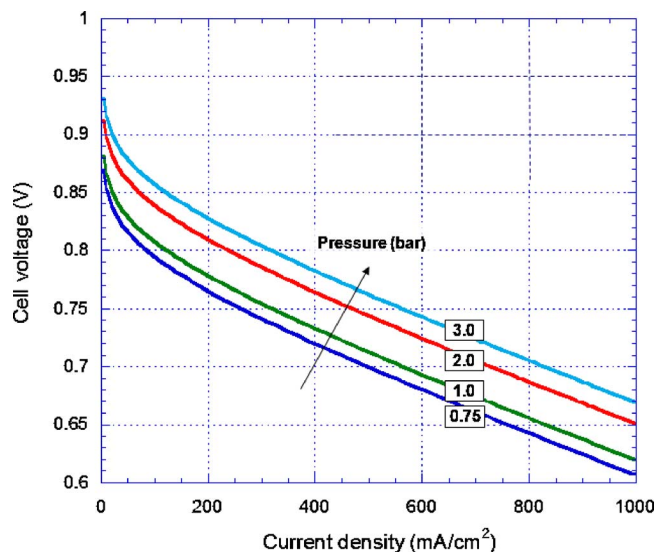


Fig. 3 Cell polarization curves at variable pressure (data for GORE® Primea Series 56 membranes, $T=75^\circ\text{C}$ Ref. [16]).

The FC generates direct current electrical energy with an efficiency proportional to its voltage. The efficiency is positively affected by pressurized operation, with a gain proportional to the operating pressure, while it decreases by increasing the cell current density. The model calculates the cell electric power production, heat generation, and efficiency together with the thermodynamic properties and chemical composition of the inlet and outlet flows, as a function of the cell operating conditions (temperature, pressure, current density, fuel, and oxidizer composition and utilization factors).

The amount of hydrogen that permeates and reacts with oxygen is calculated by multiplying the mass stream at the anode inlet with the fuel utilization factor. In the same way, the inlet air flow is estimated based on the air utilization factor. The anode outlet mass flow is computed as the difference between the inlet mass flow and the hydrogen permeated; the cathode outlet stream is the sum of the cathode inlet air, the water for cooling, and the hydrogen permeated.

The cell voltage V_c is estimated based on the cell current density i_c by means of the following equation [13]:

$$V_c = A + B \log_{10} i_c + C i_c \quad (1)$$

This formula does not consider the concentration losses, because in this study we assume that the fuel cell operating conditions always fall in the linear portion of the polarization curve, where the dominant effect is a linear resistance loss. The parameters A , B , and C are function of temperature and pressure and they can be expressed by the following equations [14,15]:

$$A = a + b \log_{10} P \quad (2)$$

$$B = c + dT \quad (3)$$

Table 3 Constants in Eqs. (1)–(4)

a	0.779
b	0.104
c	0.0324
d	-2.21×10^{-4}
e	-1.50
f	3.85×10^{-3}

Table 4 PEM model assumptions

$\Delta p/p$ air/fuel side	1%
Heat loss	1%
dc-ac efficiency	94%
Fuel utilization factor U_f	100%
Air utilization factor U_a	50%
Current density i_c	0.4 A/cm ²
Fuel composition	100% H ₂

$$C = e + fT \quad (4)$$

The constants a – f of the equations are calibrated by interpolation of experimental data for state-of-the-art PEM membranes (Fig. 3). The final equation, whose constants are reported in Table 3, allows us to reproduce experimental results with an average voltage error below 1% in the regions of interest.

Based on the cell voltage, the stack electric power is calculated by

$$P_{el} = 2 \times F \times N_{H_{2,p}} \times V_c \quad (5)$$

where $N_{H_{2,p}}$ (mol/s) are the moles of hydrogen permeated from anode to cathode. It is then possible to find the cell active area, A_c , as the ratio between power output (P_{el}) and the product of current density and cell voltage ($i_c V_c$).

The amount of water injected for cooling is calculated iteratively with respect to the energy balance of the system, reaching an assigned value of the cathode and anode outlet temperature (75°C). Compositions are calculated based on the quantity of hydrogen permeated.

The following table (Table 4) shows other fuel cell simulation assumptions. Fuel is assumed here to come from pressurized tanks, so that no fuel compressor is required.

3.2 Compressor and Other Components. The system layout includes a compressor, with the function of raising the cell pressure up to a desired value, and may include a turbine. These components work with maximum pressure ratios in the range 3.5–4.5, similar to those of radial turbomachines used for gas microturbines [17–19]. However, the air mass flow rate handled in the PEM system considered here is rather low (below 0.1 kg/s, i.e., that of a few kilowatt microturbine), suggesting the necessity to adopt very high speed components [20,21], comparable to those used for the turbochargers of the car industry. The assumptions used for their simulation, together with those of other plant components (heat exchangers), are shown in Table 5 [22–24].

Based on the aircraft operating conditions considered above, the compressor system has to deal with a large variation of pressure ratio (1.2–4.5) and an extremely wide variation of inlet volumetric air flow rate, the latter yielding a sixfold variation of corrected mass flow at compressor inlet (Eq. (6)) going from ground operation to high altitude flight.

$$m_r = m_{in} \frac{\sqrt{T/T_{ref}}}{p/p_{ref}} \quad (6)$$

The typical operating range for centrifugal compressors allows a corrected mass flow variation around 1:3 between the minimum and maximum pressure ratios requested here [22]; this consideration suggests that the compressor system has to be designed with two parallel units, the first operating at ground and low altitudes, and the second added at high altitude when the inlet air volumetric flow rate becomes too large.

4 Plant Configurations and Thermodynamic Results

The proposed plant configuration is shown in Figs. 4(a)–4(c) with the corresponding energy balances and with the thermodynamic conditions of all the relevant cycle points. The analysis of the complete power cycle is made with a modular simulation code

Table 5 Compressor and other component model assumptions (cases A–C are presented in Sec. 4)

Compression system	
Design conditions (cruise)	
Pressure ratio	3.0
Mass flow at compressor inlet (kg/s)	0.07
Corrected mass flow (Eq. (6), kg/s)	0.274
Compressor isentropic efficiency [6]	0.76
Turbine isentropic efficiency [1]	0.82
Operating range	
Pressure ratio	1.2–4.4
Mass flow at compressor inlet (kg/s)	0.06–0.09
Corrected mass flow (Eq. (6), kg/s)	0.07–0.46
Combustor	
Combustor $\Delta p/p$ (air side, Case C)	3%
Combustion efficiency (Case C)	0.96
Mechanic and electric losses	
Organic efficiency	0.92 (A,B)–0.97 (C)
Electric motor efficiency	0.85 (A)–0.81 (B)
Heat exchangers	
Minimum ΔT (°C)	10
$\Delta p/p$ hot/cold side	1%
Heat loss	1%

(gs) already described in previous works and tested on a wide variety of gas turbine and fuel cell cycles [25–27].

The fuel cell is designed to work at a given current density (0.4 A/cm², Table 4) at cruise conditions, where the system air mass flow rate is adjusted to achieve the desired power output. The remaining operating conditions are calculated within the hypothesis of keeping the same cell active surface A_c and changing the current density (influencing the cell voltage according to Eq. (1)) to reach the same power output.

4.1 Base Case. The base case arrangement (A) is shown in Fig. 4(a). The air flow enters the system from the intake (1), where speed is turned into pressure by a diffuser, and then it is compressed up to the pressure required by the FC. After compression, the air flow (3) shall be cooled to the temperature required by the FC with a heat exchanger, for instance, going from 95°C to 100°C down to 80°C. At the inlet of the cathode (5), air is mixed with water at about 55°C (6) for cell humidification, resulting in a further reduction of temperature. Hydrogen (4) feeds the PEM anode after being depressurized to the same pressure of the air flow¹. The water required for humidification is separated by condensation from the cathode exhaust stream and recycled; the remaining exhausts are vented in the atmosphere (7). Thermodynamic properties and composition of the main streams are showed in Table 6.

Preliminary optimization of the cell operating pressure has shown, with all the operating conditions of Table 2, that there is no practical gain to operate the fuel cell at higher pressure when the external ambient pressure is lower than the minimum pressure level considered above (0.8 bar): It always happens that the power required to drive the compressor is much higher than the gain obtained with a higher cell voltage and cell power output [24]. Consequently, cell pressure is set at a minimum of 0.8 bar during flight, while at higher ambient pressure conditions (i.e., ground conditions) the system is only slightly pressurized at 1.2 bars to sustain internal pressure drops. The system energy balances are

¹Fuel preheating at 15°C is necessary when the tank temperature is too low. It is accomplished with a small heat exchanger (not shown in figures for simplicity), recovering heat from the cell cooling loop.

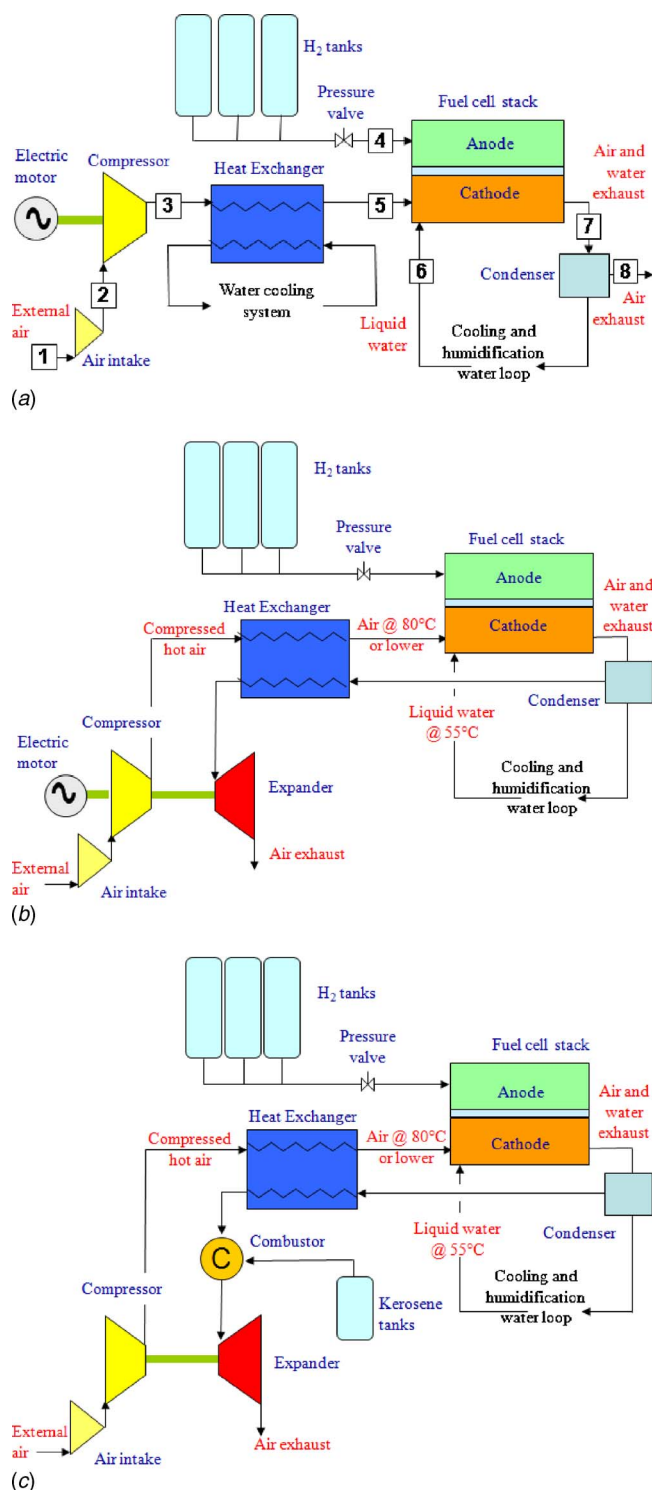


Fig. 4 (a) Schematic layout of the base case. (b) Schematic layout of the case with turbocharger. (c) Schematic layout of the case with combustor and turbocharger.

presented in Table 7. They indicate a design efficiency of 43.5% at cruise conditions, while the efficiency is 52.5% during ground operation, where the compressor consumption becomes negligible.

A possible improvement of this configuration would be to exploit the expansion of the vented gases (point 8 in Fig. 4(a)) in a turboexpander; however, direct expansion is not feasible because the low turbine inlet temperature would easily lead to frost forma-

tion in the expander. It could be possible to stop the turbine expansion at a higher pressure than atmospheric in order to avoid this problem, but the power gain would be too low to justify the complexity added to the system. The solution of adopting a turboexpander becomes feasible only changing the system layout as presented in the following cases.

4.2 Case With Turbocharger. In the second case (B), shown in Fig. 4(b), the cooling of compressed air is done with the cell exhaust gases. This solution allows us to avoid introducing an additional cooling flow, and the temperature of the gases becomes acceptable for a turbine expansion. The resulting TIT is anyway very low, so that expansion power remains lower than compression power; therefore, an electric motor is required to cooperate in driving the compressor. However, the electric power consumption of the motor is significantly lower than in Case A, giving the possibility to achieve a higher system efficiency. The system net electrical efficiency reaches 50.5% at cruise conditions (Table 8), with an operating pressure higher than in Case A.

The system optimal operating pressure is set to maximize the efficiency, as shown in Fig. 5 for the case of cruise conditions, where the optimized pressure of 1.2 bars corresponds to a compressor pressure ratio $\beta=4.5$.

At the other two operating conditions, the effect of pressure is different: Efficiency decreases with pressure in the worst case, due to the extremely low initial pressure at compressor inlet, then the PEM is operated at 0.8 bar (and $\beta \sim 4.5$). At ground conditions, pressurization gives instead some advantages, with the efficiency reaching a flat maximum at about 2.5 bars ($\beta \cong 2.5$)²

Although the electrical efficiency is very high, the system layout is complicated by the concept of powering the compressor partly by the turbine and partly by the electric motor, a solution which would probably face significant control issues under the very different operating points required by this application. However, it should be noted that such arrangement is, in principle, similar (except for the direction of the power flow) to the one commonly used in gas turbines, where the turbine drives the compressor and the alternator; moreover, the electric motor could be used during startup and other transient operation procedures.

4.3 Case With Combustor and Turbocharger. Case C is similar to the previous one, with a combustor added to make the turbocharger always self-sustained (Fig. 4(c)). The system layout avoids using the electric motor³, but the combustor consumes additional fuel; aiming to reduce the hydrogen consumption, we have assumed here to use the same jet fuel already onboard the aircraft to feed this combustor.

In all cases, the system efficiency remains between that of Cases A and B, reaching 48.7% under cruise conditions (Table 9). The cell active area is about 6% lower than in Case B and 20% lower than in Case A, allowing significant savings on the PEM cost, because the fuel cell does not have to sustain the consumption of the electric motor.

The effects of cell pressure on electrical efficiency and the resulting TIT are shown in Figs. 6 and 7. At cruise conditions, results are similar to what has been found in Case B. The required TIT is always very low (i.e., below 550 K), so the combustor should be operated with an extremely large excess air, with the possibility of achieving low NO_x emissions.

At ground conditions, the efficiency rises up to $\beta \cong 4$, but the majority of the gain is already achieved at $\beta=2-3$; setting the operating point within this range allows us also to minimize the TIT.

On the other hand, the very low TIT remarks that the gas cycle,

²Above this pressure level pressurization would require a substantial increase of the water spray necessary to sustain the DWI cooling concept, as discussed at Sec. 3.1.

³This yields also an increase of mechanical efficiency thanks to the absence of a gearbox.

Table 6 Stream data for Case A (Fig. 4(a)), cruise conditions

	T (°C)	P (bar)	m (g/s)	Molar fractions (%)					
				Ar	CO ₂	H ₂	H ₂ O	N ₂	O ₂
1	-56.5	0.23	79.2	0.92	0.03	—	1.03	77.28	20.73
2	-25.2	0.27	79.2	0.92	0.03	—	1.03	77.28	20.73
3	95.4	0.81	79.2	0.92	0.03	—	1.03	77.28	20.73
4	15	0.81	1.15	—	—	100	—	—	—
5	80	0.80	79.2	0.92	0.03	—	1.03	77.28	20.73
6	55.4	0.80	25.1	—	—	—	100	—	—
7	75	0.79	105.5	0.57	0.018	—	44.99	47.98	6.44
8	53.8	0.75	80.4	0.83	0.03	—	19.72	70.02	9.39

Table 7 Energy balances for Case A (PEM $A_c=27.5$ m²)

	Cruise	Worst	Ground
PEM pressure (bar)	0.8	0.8	1.2
Pressure ratio β	3.0	4.4	1.2
Cell voltage V_c (V)	0.700	0.685	0.722
Cell current density (A/cm ²)	0.400	0.461	0.333
m_{air} (kg/s)	0.079	0.091	0.066
PEM fuel heat input ($m_{fuel,PEM} \times LHV$) (kW)	137.7	158.7	114.7
$P_{el,PEM}$ (kW)	72.36	81.52	62.15
$P_{el,compressor}$ (kW)	12.36	21.52	2.15
Electric efficiency η_{el} (%)	43.57	37.82	52.31

Table 8 Energy balances for Case B (PEM $A_c=23.7$ m²)

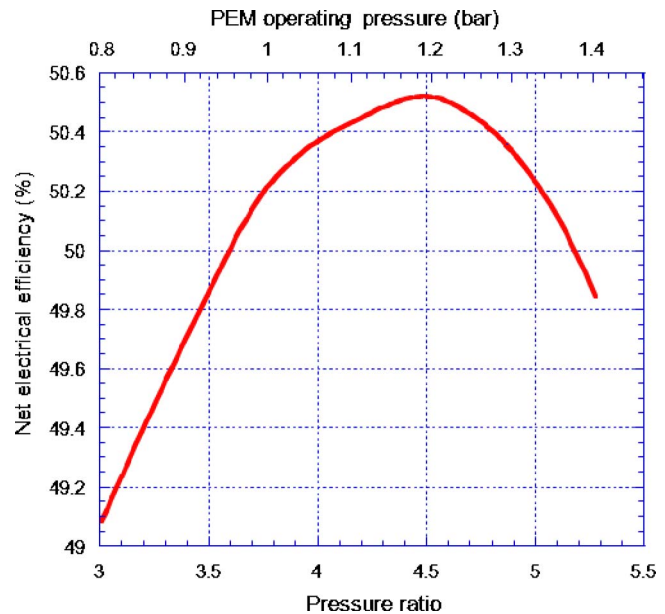
	Cruise	Worst	Ground
PEM pressure (bar)	1.2	0.8	2.5
Pressure ratio β	4.5	4.4	2.6
Cell voltage V_c (V)	0.719	0.695	0.757
Cell current density (A/cm ²)	0.400	0.421	0.381
m_{air} (kg/s)	0.068	0.072	0.065
PEM fuel heat input ($m_{fuel,PEM} \times LHV$) (kW)	118.7	125.1	113.1
$P_{el,PEM}$ (kW)	64.00	65.20	64.21
$P_{el,motor}$ (kW)	4.00	5.20	4.21
$P_{compressor}$ (kW)	12.11	13.26	7.89
$P_{turbine}$ (kW)	9.13	9.39	4.76
Losses (mech., el.) (kW)	1.02	1.33	1.08
Electric efficiency η_{el}	50.53	47.98	53.04

although self-sustained, has poor thermodynamic quality; this turns into the efficiency decrease—in all operating points—with respect to Case B.

4.4 Comparisons. The energy analysis shows that both Cases B and C, relying on a turbocharger to drive the compressor, achieve better electrical efficiency and reduce the electric power output required to the PEM with respect to Case A. The system layout of Cases B and C is of course more complicated, but given that the specific costs of the PEM are much higher than those of the expander, it is possible that these solutions are preferable also from an economic point of view⁴

Among the two favored cases, plant B reaches maximum efficiency, also featuring zero NO_x and CO emissions, thanks to the absence of any conventional combustor.

⁴A detailed economic analysis, which goes beyond the scope of this paper, should be carried out to investigate this aspect.

**Fig. 5 Electrical efficiency of Case B as a function of pressure at cruise conditions****Table 9 Energy balances for Case C (PEM $A_c=22.2$ m²)**

	Cruise	Worst	Ground
PEM pressure (bar)	1.2	0.8	2.5
Pressure ratio β	4.5	4.4	2.6
Cell voltage V_c (V)	0.719	0.697	0.757
Cell current density (A/cm ²)	0.400	0.412	0.380
m_{air} (kg/s)	0.064	0.066	0.061
GT TIT (K)	546	593	692
PEM fuel heat input ($m_{fuel,PEM} \times LHV$) (kW)	111.3	114.7	105.7
GT fuel heat input ($m_{fuel,GT} \times LHV$) (kW)	11.8	15.5	21.6
$P_{el,PEM}$ (kW)	60.0	60.0	60.0
$P_{compressor}$ (kW)	11.36	12.16	7.37
$P_{turbine}$ (kW)	11.71	12.54	7.60
Losses (mech.) (kW)	0.35	0.38	0.23
Electric efficiency η_{el}	48.73	46.09	47.12

It is interesting to compare the best PEM configurations (Cases B and C) with a conventional APU. Table 10 shows the energy balances of the plants: both PEM cases have of course a much better efficiency, which allows significant advantages in terms of

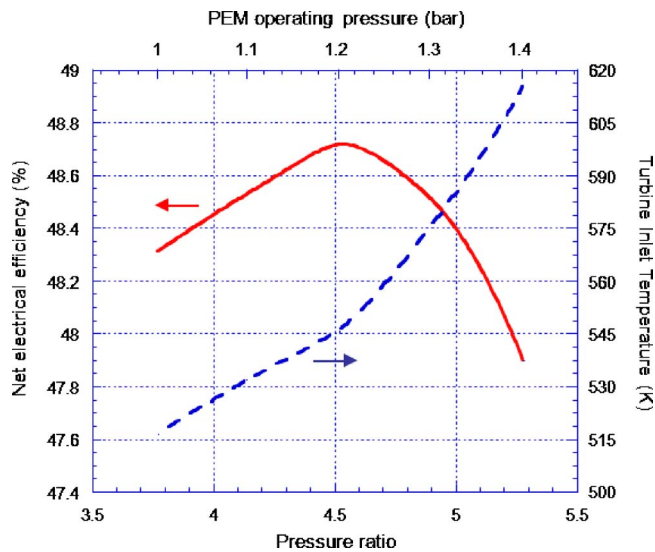


Fig. 6 Electrical efficiency and TIT of Case C as a function of pressure for cruise conditions

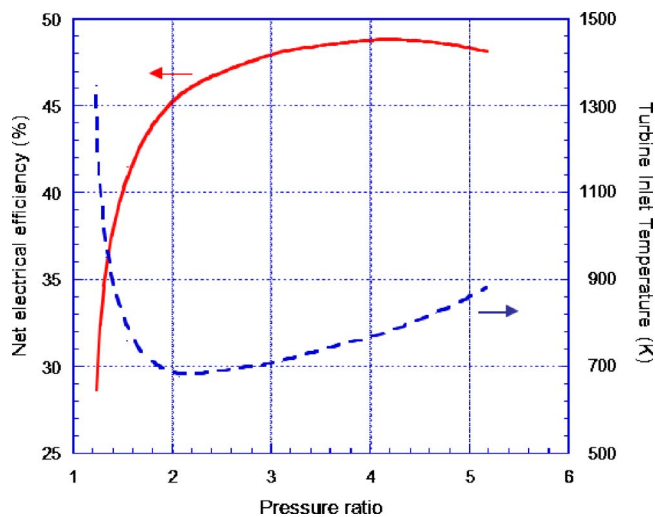


Fig. 7 Electrical efficiency and TIT of Case C as a function of pressure for ground conditions

reducing the weight of the fuel consumed during flight⁵

By the point of view of water consumption, the amount of water sprayed at the PEM cathode for cell humidification and cooling (by partial evaporation and sensible heat exchange) ranges between 375 g/s and 353 g/s for Cases B and C at cruise conditions (Table 10), and can be entirely recovered by condensation of the system exhausts.

For comparison, the alternative of cooling with a separate water circuit would require 624.5 g/s for scenario B and 588.3 g/s for scenario C (with heat exchange only through sensible heat, under the same temperature differences), while reducing the amount of water to be evaporated for the saturation of the cathode flow at about 8.3 and 7.8 g/s, respectively, for Cases B and C.

6 Conclusions

This work has considered the issue of integrating a PEM fuel cell onboard an aircraft for generating a fraction of auxiliary sys-

⁵Further analysis would be required to compare the systems in terms of weight at takeoff; for instance, the PEM generator is expected to be significantly—but not extremely—heavier than a conventional APU.

Table 10 Energy balances for a conventional turbine APU ($\beta=3$, TIT=1073 K) and for the PEM Cases B and C (cruise conditions)

Energy balances	PEM B	PEM C	GT
System net power output (kW)	60.0	60.0	60.0
PEM fuel heat input	118.7	111.3	0.0
$(m_{\text{fuel,PEM}} \times \text{LHV})$ (kW)	—	—	—
GT fuel heat input	—	11.8	349.3
$(m_{\text{fuel,GT}} \times \text{LHV})$ (kW)	—	—	—
Hydrogen consumption (kg/h)	3.56	3.34	—
Jet fuel consumption (kg/h)	—	0.99	21.43
m_{air} (kg/s)	0.068	0.064	0.30
Stack outlet temperature (K)	280	391	836
Electric efficiency η_{el}	50.53	48.73	17.75

tems electric consumption. Calculations have been performed with a model that takes into account the effects of temperature and pressure on the cell efficiency, optimizing the fuel cell operating point at variable flight conditions. Different system architectures have been considered, where the FC is fed with hydrogen as fuel and compressed air taken from the external surroundings as oxidizer: the first (Case A) with the air fed to the FC by an electrically driven compressor, the other (Cases B and C) relying on a turbocharger to drive the compressor, reaching better electrical efficiency and reducing the size of the PEM. Optimized pressure ratios have been found, with the cell operating pressure ranging from 0.8 bar to 2.5 bars. In all cases, the proposed system yields relevant fuel savings with respect to a conventional gas-turbine APU, with the distinctive advantage of achieving zero NO_x emissions in the most efficient configuration, where net electrical efficiency exceeds 50% at aircraft cruise conditions.

Acknowledgment

The reported research was conducted at the Department of Energy of Politecnico di Milano within the framework of a program agreement for M.Sc. stages active with Airbus. The authors wish to thank Professor A. Coghe of Politecnico di Milano and Dr. Guenter Walper of Airbus Deutschland for their cooperation.

Nomenclature

A_c	= cell active area (cm^2)
F	= Faraday's constant (96 439 C/mol of electrons)
i_c	= cell current density (A/cm^2)
m	= mass flow rate (kg/s)
p	= pressure (Pa)
P_{el}	= electric power (MW)
Q_{th}	= thermal power (MW)
T	= temperature ($^{\circ}\text{C}$ or K)
U_a	= cell air utilization factor: $U_a = \text{O}_{2,\text{consumed}} / \text{O}_{2,\text{inlet}}$
U_f	= cell fuel utilization factor: $U_f = \text{H}_{2,\text{consumed}} / \text{H}_{2,\text{inlet}}$
V_c	= cell voltage (V)
β	= pressure ratio
η_{el}	= electric efficiency (LHV base)

Acronyms

dc/ac	= direct/alternating current
FC	= fuel cell
GT	= gas turbine
LHV	= lower heating value (kJ/kg)
PEM	= polymer electrolyte membrane fuel cell
TIT	= turbine inlet temperature

References

- [1] Eelman, S., Pozo del Poza, I., and Kreig, T., 2004, "Fuel Cell APU'S in Commercial Aircraft-An Assessment of SOFC and PEMFC Concepts," 24th International Congress of Aeronautical Sciences (ICAS).
- [2] Daggett, D. L., Eelman, S., and Kristiansson, G., 2003, "Fuel Cell APU for Commercial Aircraft," AIAA/ICAS International Air and Space Symposium and Exposition, OH, July.
- [3] Anon, 2005, "6th European Framework Program, PROPAIR: Processing of Kerosene for PEM Fuel Cell Applications for Aircraft," Airbus Internal Document, Part B, July.
- [4] Anon, 2005, "6th European Framework Program, CELINA: Fuel Cell Integration in a new Configured Aircraft," Description of Work-Airbus Internal Documents, February.
- [5] Anon, 2006, "787 Special-Electric Dream," *Flight International*, pp. 58–59; <http://www.flightglobal.com/articles>
- [6] Barchewitz, L. P., and Seume, J. R., 2006, "Conceptual Analysis of Air Supply Systems for In-Flight PEM-FC," ASME Paper No. 2006-GT-90688.
- [7] Cunningham, J. M., Hoffman, M. A., and Friedman, D. J., 2001, "A Comparison of High-Pressure and Low-Pressure Operation of PEM Fuel Cell Systems," University of California, SAE Engineering Congress.
- [8] Anon, 2005, "Fuel Cell Systems for Emergency Power Supply Onboard of an Aircraft," European Consortium for Advanced Training in Aerospace, ECATA, Airbus Internal Document, Final Report.
- [9] Anon, 2006, "Avanti and Forza PEM Modules," Nuvera website: <http://www.nuvera.com>
- [10] Nuvera Europe Technical Management and Experimental Laboratories, 2006 (private communication).
- [11] Anon, 2006, *Fuel Cell Handbook*, 7th ed. U.S. Department of Energy, Morgantown, WV.
- [12] S., Campanari, E., Macchi E., and A., Silva, 2005, *Micro-Cogeneration With Natural Gas*, Polipress, Milan, Italy (in Italian).
- [13] Larminie, J., and Dicks, A., 2003, *Fuel Cell Systems Explained*, Wiley, New York.
- [14] Kulp, G. W., 2001, "A Comparison of Two Air Compressors for PEM Fuel Cell Systems," MS thesis, Mechanical Engineering, Virginia.
- [15] Pratt, J., Brouwer, J., and Samuelsen, G., 2003, *Experimental Evaluation and Computer Simulation of an Air-Breathing PEM Fuel Cell at Aircraft Flight Altitudes*, National Fuel Cell Research Centre, Irvine, CA.
- [16] Anon, 2006, "Primea Series 56 Membranes," Website: www.gore.com.
- [17] Campanari, S., 2000, "Full Load and Part-Load Performance Prediction for Integrated SOFC and Microturbine Systems," ASME J. Eng. Gas Turbines Power, **122**, pp. 239–246.
- [18] O'Brien, P., 1998, "Development of a 50-Kw, Low-Emission Turbo-Generator for Hybrid Electric Vehicles," ASME Paper No. 98-GT-400.
- [19] Jones, A. C., 1994, "Design and Test of a Small, High Pressure Ratio Radial Turbine," ASME Paper No. 94-GT-135.
- [20] Rodgers, C., "25 to 5 kWe Microturbine Design Aspects," ASME Paper No. 2000-GT-0626.
- [21] Gerendas, M., and Pfister, R., 2000, "Development of a Very Small Aero-engine," ASME Paper No. 2000-GT-536.
- [22] Balje, O. E., 1981, *Turbomachines-A Guide to Design, Selection and Theory*, Wiley, New York.
- [23] Perdichizzi, A., and Lozza, G., 1987, "Design Criteria and Efficiency Prediction for Radial Inflow Turbines," ASME Paper No. 87-6T-231.
- [24] Beretti, A., 2006, "Analysis of Turbocharged PEM Fuel Cell Systems for Civil Aircraft Onboard Power Production," MS thesis, Politecnico di Milano.
- [25] Consonni, S., Lozza, G., Macchi, E., Chiesa, P., and Bombarda, P., 1991, "Gas-Turbine-Based Advanced Cycles for Power Generation-Part A: Calculation Model," *International Gas Turbine Conference*, Vol. III, Yokohama, pp. 201–210.
- [26] Campanari, S., and Macchi, E., 1998, "Thermodynamic Analysis of Advanced Power Cycles Based Upon Solid Oxide Fuel Cells, Gas Turbines and Rankine Bottoming Cycles," ASME Paper No. 98-GT-585.
- [27] Chiesa, P., and Macchi, E., 2004, "A Thermodynamic Analysis of Different Options to Break 60% Electric Efficiency in Combined Cycle Power Plants," ASME J. Eng. Gas Turbines Power, **126**, pp.770–784.